

## **The list of changes made in the manuscript**

1. line 12: add the full name of GNSS
2. line 21: add the full name of RMS
3. line 33: add a citation about iono-free combination techniques
4. line 37~40: rewrite the phrase
5. line 41~99: short the description and make some corrections
6. line 105: correct 'girds' to 'grids'
7. line 113: correct 'theoretically' to 'practical'
8. line 124: add the dot
9. line 144~145: add the extended form of doy
10. line 169~170: add the explanation for error bars
11. line 173: remove 'and'
12. line 193~196 and line 205~207: add the introduction of the GZTD model
13. line 200: replace 'Different from' with 'In contrast with'
14. line 212~216: rephrase the sentence to avoid confusion
15. line 247: remove 'in theory'
16. line 248: add 'The'
17. line 297~301: rewrite the sentence and add two citations
18. line 310~313: add the strategy of IGS sites selection
19. line 363: replace 'reduce' with 'reduction'
20. line 378: replace 'lager' with 'larger'
21. line 406: replace 'obviously' with 'substantially'
22. line 408: replace 'improve' with 'improves'
23. line 411: add the dot
24. line 412~431: rephrase the conclusions for clarity and make some corrections
25. line 493 and 495: add the full name of the first author
26. line 501~503 and 508~511: add three references

# An improved global zenith tropospheric delay model GZTD2 considering diurnal variations

YiBin Yao<sup>1,2,3</sup>, YuFeng Hu<sup>1</sup>, Chen Yu<sup>1</sup>, Bao Zhang<sup>1</sup>, JianJian Guo<sup>1</sup>

<sup>1</sup>*School of Geodesy and Geomatics, Wuhan University, 129 Luoyu Road, Wuhan 430079, China. E-mail: [ybyao@whu.edu.cn](mailto:ybyao@whu.edu.cn)*

<sup>2</sup>*Key Laboratory of Geospace Environment and Geodesy, Ministry of Education, Wuhan University, 129 Luoyu Road, Wuhan 430079, China*

<sup>3</sup>*Collaborative Innovation Center for Geospatial Technology, 129 Luoyu Road, Wuhan 430079, China*

**Abstract--**The zenith tropospheric delay (ZTD) is an important atmospheric parameter in the wide application of [global navigation satellite systems \(GNSS\)](#) technology in geoscience. Given that the temporal resolution of the current Global Zenith Tropospheric Delay model (GZTD) is only 24 h, an improved model GZTD2 has been developed by taking the diurnal variations into consideration and modifying the model expansion function. The data set used to establish this model is the global ZTD grid data provided by Global Geodetic Observing System (GGOS) Atmosphere spanning from 2002 to 2009. We validated the proposed model with respect to ZTD grid data from GGOS Atmosphere, which was not involved in modeling, as well as International GNSS Service (IGS) tropospheric product. The obtained results of ZTD grid data show that the global average Bias and [Root Mean Square \(RMS\)](#) for GZTD2 model are 0.2 cm and 3.8 cm respectively. The global average Bias is comparable to that of GZTD model, but the global average RMS is improved by 3 mm. The Bias and RMS are far better than EGNOS model and the UNB series models. The testing results from global IGS tropospheric product show the Bias and RMS (-0.3 cm and 3.9 cm) of GZTD2 model are superior to that of GZTD (-0.3 cm and 4.2 cm), suggesting higher accuracy and reliability compared to the EGNOS model, as well as the UNB series models.

**Key Words**—Zenith tropospheric delay; GGOS Atmosphere; IGS; Diurnal variation; GZTD2 model.

# 1. Introduction

Radio space-based geodesy techniques suffer from atmosphere propagation delays, of which the ionospheric delay can be largely eliminated by iono-free carrier phase combination techniques (Spilker 1980), and then the tropospheric delay becomes the main error source. In general, we project the slant delay to zenith direction with mapping function in GNSS navigation and positioning, so modeling the ZTD is a common method to reduce the tropospheric influence on signal travelling. In order to improve the accuracy and efficiency of the application in earth science based on space geodesy techniques ~~better exploit the modern development of geodetic techniques~~, a ~~more~~ reliable tropospheric delay model is required. ~~to improve the accuracy and efficiency of the application in earth science based on space geodesy techniques.~~

~~The correction accuracy of some traditional tropospheric delay models such as Hopfield model (Hopfield 1969), Saastamoinen model (Saastamoinen 1973), Black model (Black 1978), can be up to centimeter or decimeter level using the real time meteorological parameters, while these models perform poorly when using the standard atmospheric meteorological parameters. Collins and Langley (1997) established UNB series models for the promotion of U.S. Wide Area Augmentation Navigation System (WAAS). In North America, the average tropospheric zenith delay error of UNB3 model was 2 cm (Collins et al. 1998). UNB3m model estimates the wet delay using relative humidity, and the average deviation was 0.5 cm (Leandro et al. 2006; Leandro et al. 2008). EGNOS model is a tropospheric delay correction model used by European Geostationary Navigation Overlay System (EGNOS), which is established by using the  $1^{\circ} \times 1^{\circ}$  grid data generated by the European Centre for Medium Range Weather Forecasts (ECMWF) (Dodson et al. 1999; Penna et al. 2001; Ueno et al. 2001), whose correction accuracy is close to that of Hopfield and Saastamoinen model provided with meteorological measurements. Li Wei et al. (2012) established the IGGtrop global tropospheric delay empirical model using the three-dimensional parameter table from reanalysis data of National Centers for Environmental Prediction (NCEP), which considered the longitudinal changes of zenith troposphere. The accuracy was improved~~

59 significantly, but the calculation of zenith tropospheric total delay required a number of  
60 parameters. Then Li Wei et al. (2015) developed the new versions of IGGtrop named  
61 IGGtrop\_ri ( $i = 1, 2, 3$ ) by simplifying the algorithm and lowering the resolution, which  
62 substantially reduce the required numbers with a similar accuracy. Krueger (2004;2005)  
63 and Schüller (2014) obtained the annual and diurnal coefficients for underlying  
64 parameters by fitting every grid point's meteorological parameters time series of NCEP  
65 atmospheric data, and established two global tropospheric delay models—TropGrid  
66 and TropGrid2 with resolution of  $1^\circ \times 1^\circ$ . The correction accuracy of TropGrid2 is  
67 slightly better than that of IGGtrop model. Bärm et al. (2015) proposed Global pressure  
68 and temperature 2 wet (GPT2w) as an extension to GPT2 (Lagler et al. 2013) with an  
69 improved capability to determine zenith wet delays in blind model. The GPT2w model  
70 account for the annual and semiannual variations of meteorological parameters, and the  
71 validation with IGS data and an extended validation with ray-traced delays (Möller et  
72 al. 2014) show a high accuracy of about 3.6 cm for GPT2w. However, GPT2w has  
73 numerous parameters for storage like above grid models such as IGGTrop series models  
74 and TropGrid series models.

75 Some tropospheric delay models are developed to mitigate the tropospheric delay.  
76 The traditional models like the Hopfield model (Hopfield 1969), Saastamoinen model  
77 (Saastamoinen 1973) and Black model (Black 1978) require real-time meteorological  
78 data to reach a correction accuracy better than 10 cm. Given the location and time  
79 information, the UNB series models (Collins and Langley 1997, 1998; Leandro et al.  
80 2006, 2008) and EGNOS model (Dodson et al. 1999; Penna et al. 2001; Ueno et al.  
81 2001) use the empirical meteorological parameters in the form of the latitude band table  
82 to estimate the ZTD with an accuracy of about 5 cm, while the IGGTrop model (Li et  
83 al. 2012) is based on the empirical three-dimensional parameters in the form of the grids  
84 to calculate the ZTD with an accuracy of about 4 cm. However the IGGTrop model  
85 needs a large number of parameters. Then Li Wei et al. (2015) developed the new  
86 versions of IGGtrop named IGGtrop\_ri ( $i = 1, 2, 3$ ) by simplifying the algorithm and  
87 lowering the resolution, which substantially reduce the required numbers with a similar  
88 accuracy. Krueger (2004;2005) and Schüller (2014) obtained the annual and diurnal

89 coefficients for underlying parameters by fitting every grid point's meteorological  
90 parameters time series of the National Centers for Environmental Prediction (NCEP)  
91 atmospheric data, and established two global tropospheric delay models — TropGrid  
92 and TropGrid2 . The correction accuracy of TropGrid2 is 3.8 cm. Böhm et al. (2015)  
93 proposed Global pressure and temperature 2 wet (GPT2w) as an extension to GPT2  
94 (Lagler et al. 2013) with an improved capability to determine zenith wet delays in blind  
95 model. The GPT2w model accounts for the annual and semiannual variations of  
96 meteorological parameters, and the validation with IGS data and an extended validation  
97 with ray-traced delays (Möller et al. 2014) show a high accuracy of about 3.6 cm for  
98 GPT2w. However, GPT2w has numerous parameters for storage like the above grid  
99 models such as IGGTrop series models and TropGrid series models.

100 Yao et al. (2013) established a global non-meteorological parameters tropospheric  
101 delay model GZTD (Global Zenith Tropospheric Delay) based on spherical harmonics  
102 using the global zenith tropospheric delay grid data provided by Global Geodetic  
103 Observing System (GGOS) Atmosphere. The harmonic function including three terms  
104 (mean, annual and semi-annual) is used to fit the ZTD time series from 2002 to 2009  
105 for each grid, then the fitted coefficients of all the ~~grids~~grids are expanded with a 10-  
106 order and 10-degree spherical harmonics. Its modeling approach was very simple, and  
107 the overall accuracy of 4.2 cm was similar to the IGGtrop on a global scale, but the  
108 required parameters were reduced greatly to about 600. GZTD model is constructed by  
109 global daily average ZTD grid data and the model parameters were expanded with a  
110 low order spherical harmonics, whose temporal resolution is only one day in theory and  
111 spatial resolution is low.

112 In this paper, using the ZTD grid data provided by the GGOS Atmosphere, the  
113 diurnal variations in ZTD were analyzed to prove the ~~theoretically~~theoreticallypractical necessity  
114 for temporal resolution improvement of GZTD model. Then on the basis of GZTD  
115 model and taking the diurnal variations into consideration and modifying the expansion  
116 function, we developed an improved global non-meteorological parameters ZTD model  
117 — GZTD2. The data set used to establish this model is the global ZTD grid data  
118 provided by the GGOS Atmosphere from 2002 to 2009. Using ZTD grid data obtained

119 from GGOS Atmosphere and tropospheric product (Buyn et al. 2009) provided by IGS  
120 for model validation, the accuracy of GZTD2 model is superior to that of GZTD model,  
121 and this model performs much better than other commonly used models such as  
122 EGNOS model and UNB series models.

123

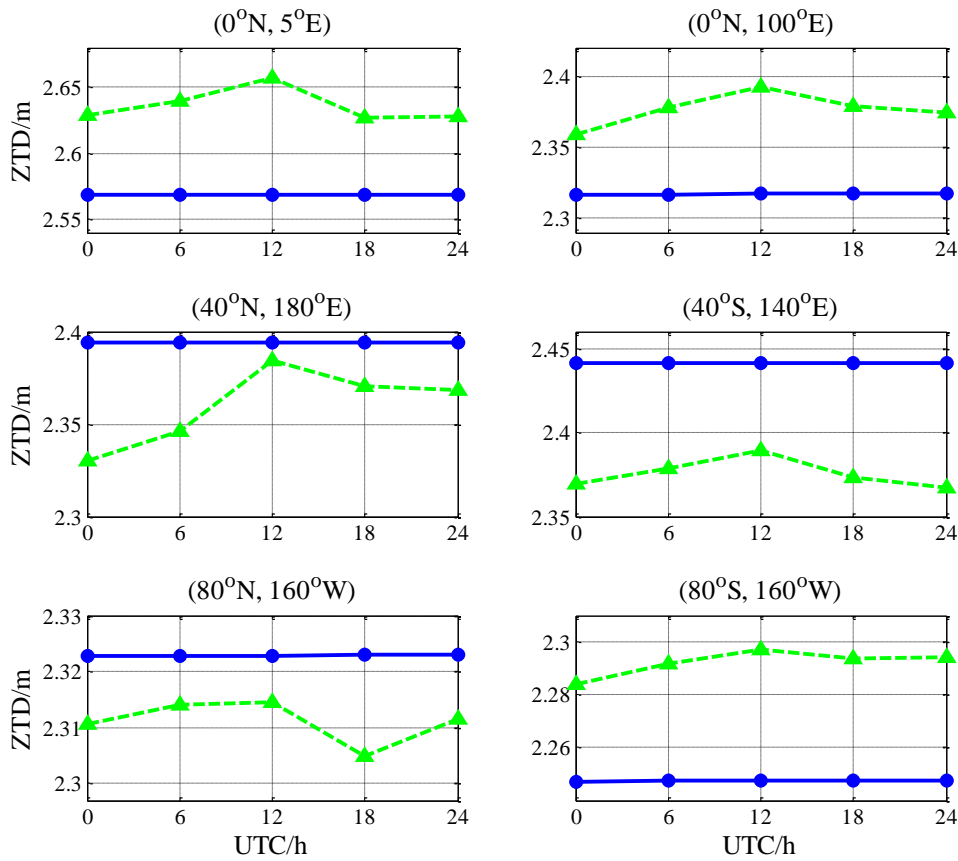
## 124 **2. The new tropospheric delay model**

125 The GGOS Atmosphere is a project that aims to establish atmospheric models,  
126 which has been carried out at Vienna University of Technology and has been funded by  
127 the Austrian Science Fund (Böhm & Schuh 2013). It provides grid data of global zenith  
128 delays (including zenith hydrostatic delay (ZHD) and zenith wet delay (ZWD)) with  
129 temporal resolution of 6 hours (0:00, 6:00, 12:00, 18:00UTC) and spatial resolution of  
130  $2.5^{\circ} \times 2^{\circ}$  (lon  $\times$  lat), which are derived from the reanalysis data (Uppala et al. 2005)  
131 provided by the ECMWF. The ZTD grid data can be obtained by simply adding up the  
132 ZHD and the ZWD at the same point and time. In this paper, the research about model  
133 establishment is based on the ZTD grid data.

### 134 **2.1 Diurnal variations in ZTD**

135 Yao et al. (2013) developed a new global zenith tropospheric delay model (GZTD),  
136 which is based on spherical harmonics without using meteorological parameters. GZTD  
137 model depends on four parameters: the day of year (doy), the latitude, the longitude and  
138 the height; and the overall accuracy is up to centimeter level. However, the algorithm  
139 of GZTD model only considers the annual and semiannual cycles in ZTD and the  
140 establishment of GZTD model is based on the daily average of global grid ZTD data,  
141 hence the temporal resolution of GZTD model is one day (24 h) in theory. We randomly  
142 selected six grid points which represent the regions in low, middle and high latitude in  
143 both the southern and northern hemispheres respectively, and applied GZTD model to  
144 estimate the ZTD at four moments (0:00,6:00,12:00,18:00 UTC) of the first day of the  
145 year (doy) in 2010, then compared the GZTD model estimations with the corresponding

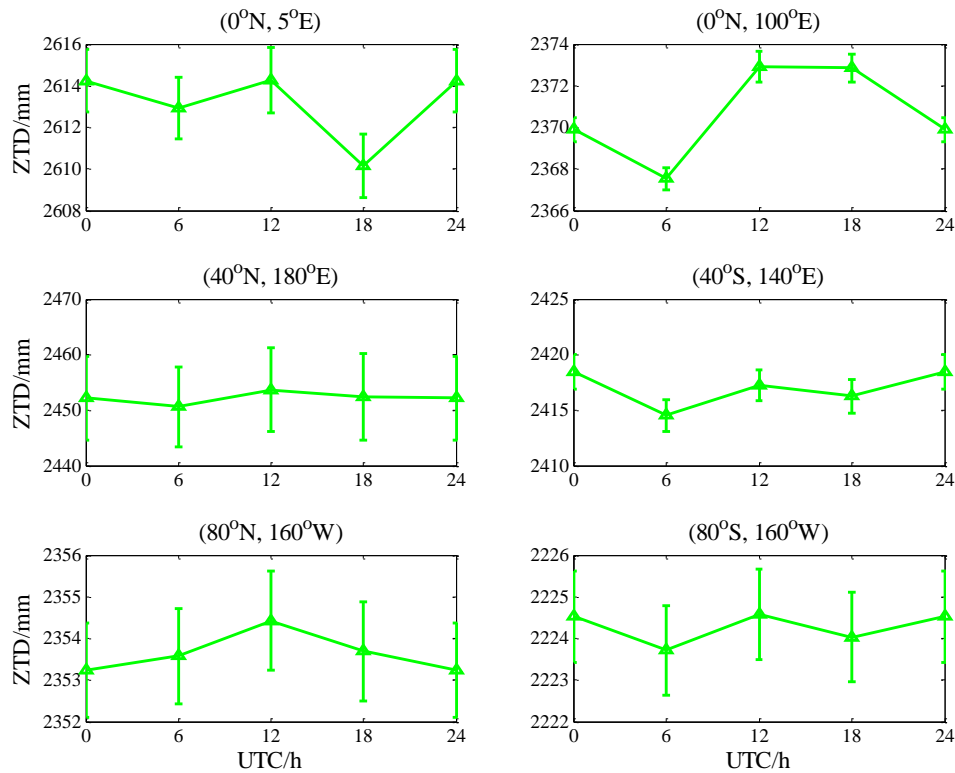
146 data from GGOS. The results are shown in Figure 1.



147  
 148 **Figure 1.** GZTD model estimates(blue ○) and corresponding GGOS grid values (green △) at the  
 149 first day of 2010

150 We can see clearly from Figure 1 that the ZTD estimates of GZTD model can  
 151 almost be fitted with a straight line parallel to the time axis which only varies about 1  
 152 mm in a single day. The real variations of GGOS grid ZTD data are mostly up to  
 153 centimeter level, which is one order larger than the variations of GZTD model estimates.  
 154 Furthermore, we calculated the mean diurnal ZTD values of these six GGOS grid points  
 155 over the whole 2010 year (Figure 2), and the significant signal of diurnal variation can  
 156 be seen at all these six grid points .We can draw a conclusion that GZTD model could  
 157 not reflect the characteristic of diurnal variations in ZTD, so the model estimations  
 158 nearly have no difference when doing calculation with real value or corresponding  
 159 integer value of the input doay. Therefore, it is necessary to improve the temporal  
 160 resolution of GZTD model to reflect diurnal variations. It should be noted that Jin et al.  
 161 (2009) has investigated the diurnal and semidiurnal variations in ZTD which obtained  
 162 from a decade of global GPS observations, and thought that the atmospheric tides were

163 the major driver of these variations after finding the general similarities of diurnal  
 164 variations between ZTD and pressure. However, the semidiurnal variations could  
 165 hardly be described because of the low temporal resolution (6 h) of GGOS ZTD data,  
 166 so we didn't consider the semidiurnal components of ZTD in modeling in the following  
 167 section.



168  
 169 **Figure 2.** Mean diurnal ZTD values of GGOS grid points with error bars denoting the standard  
 170 deviations from the average over the 2010 year

## 171 2.2 Establishment of GZTD2 model

172 According to the previous researches conducted by Jin et al. (2007) and Yao et al.  
 173 (2013), ZTD decreases exponentially with increasing height, and is featured by one-  
 174 year periodicity and half-year periodicity, and has a strong correlation with latitude.  
 175 Based on these characteristics of ZTD, we took diurnal periodic variations into  
 176 consideration to develop an improved model GZTD2. The expression of GZTD2 model  
 177 is as follows:

$$ZTD = \left[ a_0 + a_1 \cos\left(2\pi \frac{\text{doy} - a_2}{365.25}\right) + a_3 \cos\left(4\pi \frac{\text{doy} - a_4}{365.25}\right) + a_5 \cos\left(2\pi \frac{\text{hod} - a_6}{24}\right) \right] \exp(\beta h) \quad (1)$$

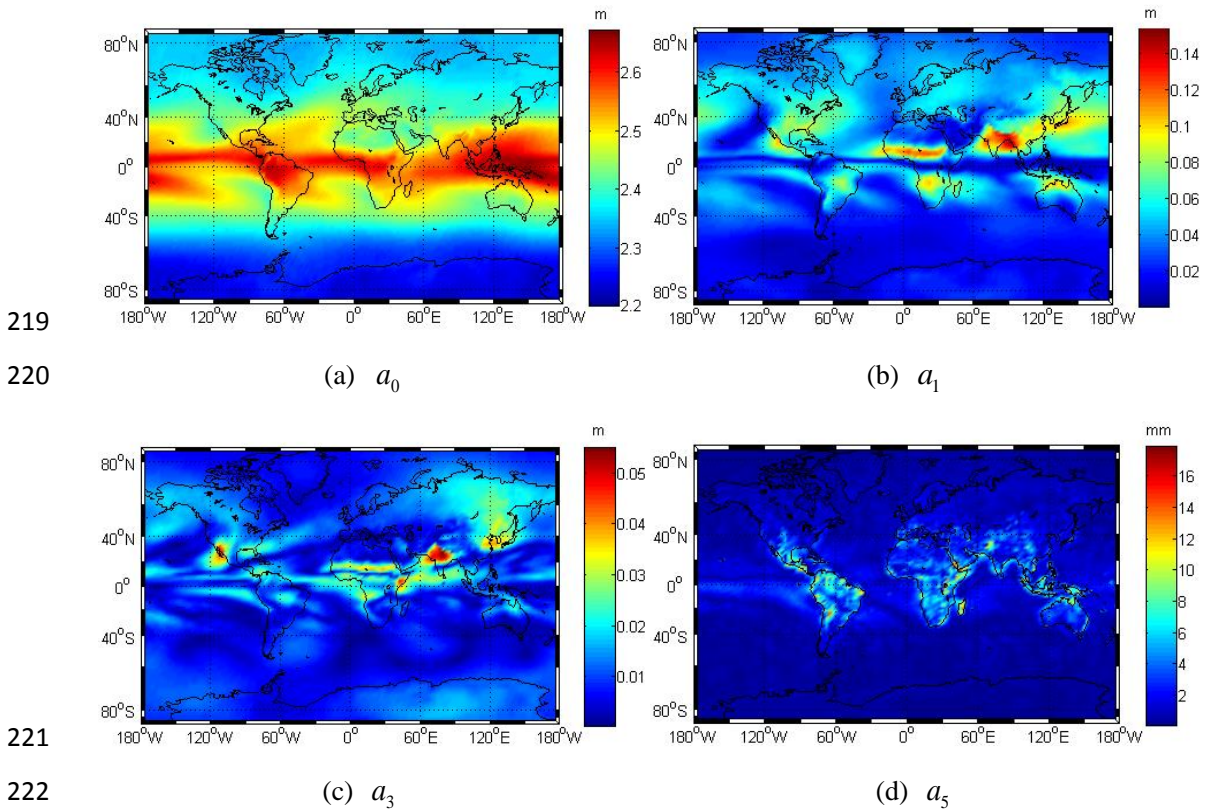
Where,

$$a_i = \sum_{n=0}^{18} \sum_{m=0}^n P_{nm}(\sin \varphi) \cdot [A_{nm}^i \cos(m\lambda) + B_{nm}^i \sin(m\lambda)] \quad (i = 0, 1, \dots, 6) \quad (2)$$

In equation(1), doy is the day of the year; hod is the UTC time;  $h$  is the height (altitude);  $a_0$  is the annual mean of ZTD on the mean sea level (MSL);  $a_1$  is the annual variation amplitude of ZTD;  $a_2$  is the initial phase of annual variation;  $a_3$  is the semiannual variation amplitude of ZTD;  $a_4$  is the initial phase of semiannual variation;  $a_5$  is the diurnal periodic variation amplitude of ZTD;  $a_6$  is the initial phase of diurnal variation;  $\beta = -0.00013137$  is the constant to reduce the ZTD at height to the MSL, which was determined by Yao et al. (2013) by fitting the global GGOS grid ZTD via exponential function with respect to height;  $P_{nm}$  ~~is~~ are the Legendre polynomials;  $\varphi$  is the latitude of grid point;  $\lambda$  is the longitude of grid point;  $A_{nm}^i$  and  $B_{nm}^i$  are the coefficients of spherical harmonics determined by least square optimization.

For each grid-point-specific ZTD time series derived from GGOS Atmosphere, we used equation (1) to fit them to temporal coefficients at MSL. Our previous GZTD model only accounts for the annual and semi-annual variations of ZTD, whose first equation is similar to equation (1) but without the fourth term (diurnal term) on the right of equation (1). However, there are seven coefficients for each grid, which need large storage space on global scale. Then referring to the idea of spherical harmonics used in GPT (Böhm et al., 2007), we used equation (2) to express the temporal coefficients (mean, annual terms et al) of all grids as a function of location (latitude, longitude and height), thus reducing the parameters. In contrast with ~~Different from~~ the GZTD model established using daily average global ZTD data, we utilized the ZTD time series data of four moments per day (0:00, 6:00, 12:00, 18:00UTC) from 2002 to 2009, provided

203 by GGOS Atmosphere, to fit ZTD values to obtain temporal variation parameters via  
 204 equation (1), then expanded these parameters with a 18-order and 18-degree spherical  
 205 harmonic function (equation (2)), respectively. The expansion equation of GZTD model  
 206 is a 10-order and 10-degree spherical harmonic function which is 8 less order and  
 207 degree than equation (2). We used this spherical harmonic function instead of the 10-  
 208 order and 10-degree function adopted in GZTD model because it is not sufficient to  
 209 apply the previous 10 order function for the expansion of the temporal variation  
 210 parameters with relatively high resolution. The number of order and degree of spherical  
 211 harmonics determine the horizontal resolution of model. However, higher order and  
 212 degree bring more parameters for model. ~~The resolution of GZTD model is about 18°~~  
 213 ~~while the diurnal variations are mostly less than 5 mm. The 10 spherical harmonics are~~  
 214 ~~too low for GZTD2 model to reflect the diurnal variations. The 10 spherical harmonics~~  
 215 ~~adopted by GZTD result in a resolution of about 18°, which is too low for GZTD2~~  
 216 ~~model to reflect the small diurnal variations.~~ To keep a balance between the resolution  
 217 and number of parameters, we used 18 spherical harmonics for GZTD2 whose  
 218 resolution is about 10°.



223 **Figure 3.** The global distribution of the annual mean ZTD on MSL (a) , the annual variation  
224 amplitude (b), the semiannual variation amplitude (c), and the diurnal variation amplitude (d)

225 Figure 3 shows the global distributions of the annual mean of ZTD on MSL and  
226 amplitude parameters after fitting by equation (1). As can be seen from Figure 3a, the  
227 coefficient  $a_0$  in low latitudes, especially, near the equator, are significantly larger  
228 than that in high latitudes, and the distribution in the Southern Hemisphere is more  
229 uniform than that in the Northern Hemisphere; These results are mostly in agreement  
230 with the results of Li et al. (2012) and Yao et al. (2013). For the sawtooth shape in the  
231  $40^{\circ}\text{N}$ - $40^{\circ}\text{S}$  region, Yao et al. (2013) found this shape appear in coastal areas and is  
232 consistent with the directions of equatorial trade winds, so they assumed that the  
233 distributions of ZTD are effected by some physical impacts such as terrains and heat  
234 circulation. Compared with the previous discovery, the sawtooth shape in Figure 3a is  
235 more evident, indicating that GZTD2 model incorporates these physical impacts.  
236 Figures 3b and 3c show the global distributions of annual amplitude and semiannual  
237 amplitude respectively, both of which are more uniform in the Southern Hemisphere  
238 than that in the Northern Hemisphere, which is probably due to the fact that most parts  
239 of the Southern Hemisphere are covered by oceans, while the Northern Hemisphere has  
240 many seacoast regions which lead to relatively complex spatial variation.

241 Figure 3d shows the global distribution of diurnal variation amplitudes. It can be  
242 seen that diurnal variation amplitudes are less than 3 mm in most parts of the world, but  
243 up to centimeter in some low-latitude equatorial areas such as Central America, South  
244 America, central Africa and tropical Asia, indicating notable diurnal variations in these  
245 areas. The distribution characteristics of diurnal variation amplitudes is similar to the  
246 results of Jin et al. (2009). So taking these diurnal variations into consideration in  
247 GZTD2 model is quite reasonable and necessary ~~in theory~~.

248 The GZTD2 model only needs doy, UTC time, latitude, longitude and height as  
249 input parameters in practical application. GZTD2 uses equation (2) to derive temporal  
250 parameters  $a_0, a_1, a_2, a_3, a_4, a_5, a_6$ , which are then entered into equation (1)  
251 together with the doy to get the ZTD at MSL. The realization of GZTD2 model is simple

252 with a few parameters, and the calculation is convenient without inputting any real-time  
 253 meteorological parameters. Table 1 summarizes the main improvements and features of  
 254 the newly suggested model compared to the GZTD model.

255 **Table 1.** Improvements of GZTD2 with respect to GZTD

	GZTD	GZTD2
Data	Daily average ZTD grid data from GGOS: 2002~2009	ZTD grid data with a resolution of 6 h from GGOS: 2002~2009
Representation	Spherical harmonics up to degree 10 and order 10	Spherical harmonics up to degree 18 and order 18
Temporal variability	Mean, annual, and semi-annual terms	Mean, annual, semi-annual and diurnal terms
Horizontal resolution	About 18 °	About 10 °

256

### 257 3. Validation and Analysis of GZTD2 model

258 To analyze the effectiveness and reliability of the new model and verify its  
 259 accuracy and stability on global scale, as well as to compare it with the GZTD model,  
 260 this section will exploit some data sources to conduct model validation. Two kinds of  
 261 data sources are used here, the first is ZTD grid data from GGOS Atmosphere which is  
 262 not used in modeling. The other is tropospheric product data provided by IGS. The  
 263 accuracy is characterized with the average deviation (Bias) and root mean square (RMS)  
 264 which are usually used for model validation (Yao et al., 2013; Li Wei et al., 2015; Böhm  
 265 et al., 2015). The expressions of Bias and RMS are:

$$266 \quad Bias = \frac{1}{n} \sum_{i=1}^n (ZTD_i^M - ZTD_i^0) \quad (3)$$

$$267 \quad RMS = \sqrt{\frac{1}{n} \sum_{i=1}^n (ZTD_i^M - ZTD_i^0)^2} \quad (4)$$

268 Where  $ZTD_i^M$  is the value estimated by model and  $ZTD_i^0$  is the reference value.

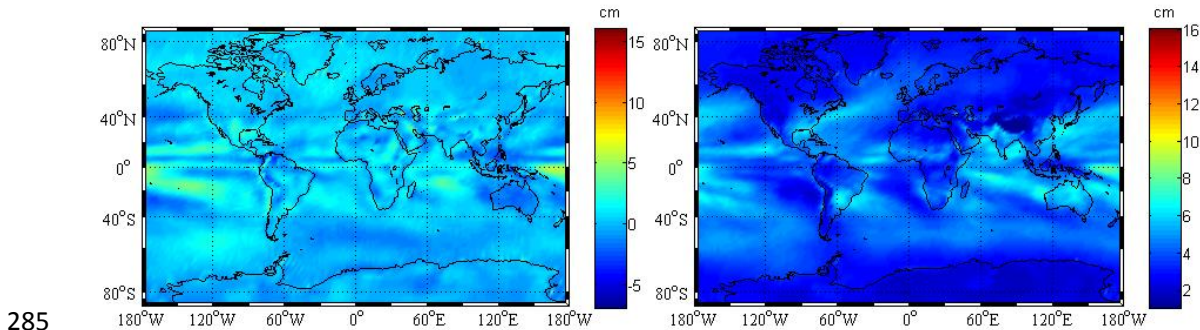
269 **3.1 Validation with GGOS Atmosphere ZTD grid data**

270 Data provided by GGOS Atmosphere from 2002 to 2009 are involved in modeling,  
 271 so we used the data of 2010 to test it. Since the resolution of ZTD grid data is  $2^\circ \times 2.5^\circ$ ,  
 272 the total number of grid points is 13,104. Treating the ZTD data at 0:00, 6:00, 12:00  
 273 and 18:00 UTC of everyday on each grid point as the reference values, we calculated  
 274 the bias and RMS of GZTD2, GZTD, EGNOS, UNB3 and UNB3m models. Statistical  
 275 analyses are shown in Table 2.

276 **Table 2.** Modeling errors of different models validated by GGOS data

	Bias (in cm)			RMS (in cm)		
	Mean	Min	Max	Mean	Min	Max
GZTD2	0.2	-3.7	6.2	3.8	0.9	8.3
GZTD	0.2	-5.4	8.0	4.1	1.1	9.5
UNB3m	3.3	-7.2	16.0	6.4	1.3	16.5
UNB3	4.5	-7.0	16.7	7.0	1.1	16.9
EGNOS	4.5	-9.6	17.7	7.2	1.0	18.1

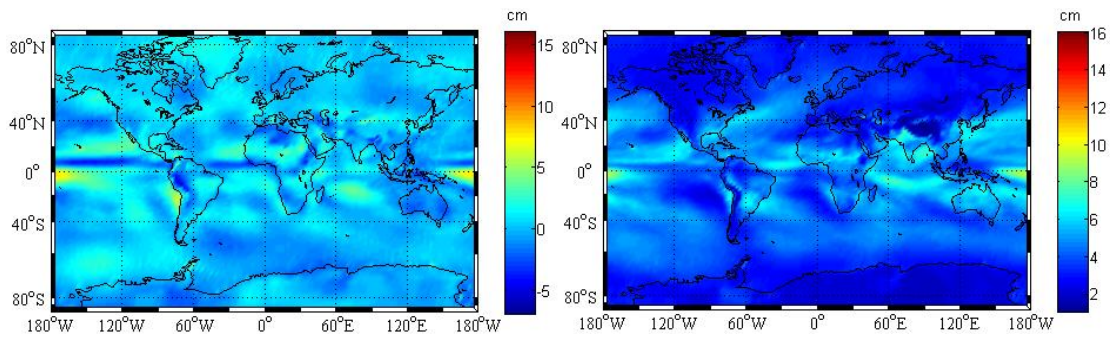
277 As can be seen from Table 2, for the total 13104 points involved in the global  
 278 validation, GZTD2 model's mean Bias is 0.2 cm with a maximum of 6.2 cm, and the  
 279 average of RMS is 3.8 cm with a maximum of 8.3 cm, significantly better than the  
 280 EGNOS and UNB series models, and the RMS is reduced by 3 mm compared with that  
 281 of GZTD model. UNB3m model's accuracy is about 1 cm better than UNB3 and  
 282 EGNOS models, so we only chose UNB3m as the representative of commonly used  
 283 model in our following comparison analysis. Figure 4 shows the global distributions of  
 284 Bias and RMS of the three models.



286

GZTD2 Bias

GZTD2 RMS

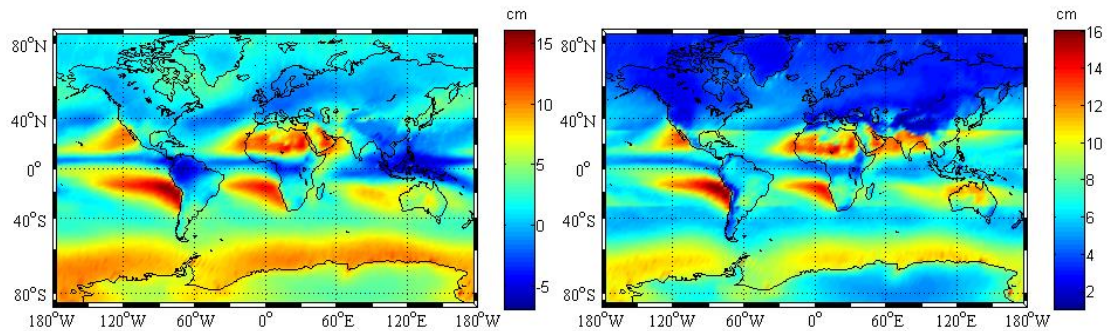


287

288

GZTD Bias

GZTD RMS



289

290

UNB3m Bias

UNB3m RMS

291

**Figure 4.** Global distribution of Bias and RMS of different models

292

As can be seen from Figure 4, compared with the other two models, the new model

293

has better accuracy in the world wide scale, and the accuracy of the areas where larger

294

errors appear improves significantly. Compared with GZTD model, GZTD2 model

295

improves the accuracy in the equator area. Obviously, all these three models have

296

suffered large errors in the Pacific Ocean near the equator and Indian Ocean. ~~These~~

297

~~areas are near the equator and may be affected by trade winds and ocean currents~~ These

298

areas are near the equator where the deep moist convection effects related to the change

299

of ZTD are more intense (Trenberth et al. 2005; Pramualsakdikul et al. 2007), so the

300

climateweather change in these areas are more complex compared with other areas,

301

resulting in difficulty for modelling tropospheric delay. In addition, GZTD2 and GZTD

302

model are comparable in Northern and Southern Hemispheres, but the UNB3m model's

303

accuracy is obviously lower in the Southern Hemisphere, this is because the UNB3m

304

model is based on the assumptions that tropospheric delay is symmetrical with equator

305

(Leandro et al., 2006). In fact, this assumption is not reasonable enough and the

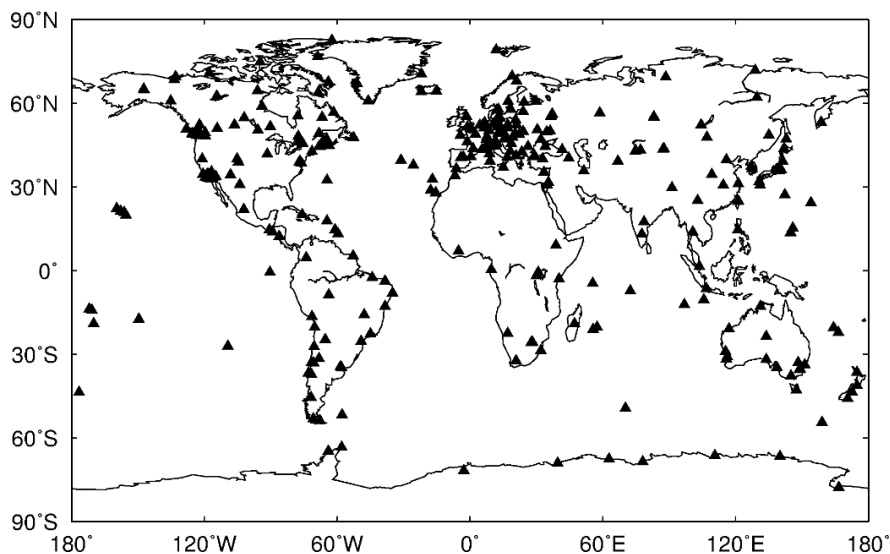
306

modeling data source are derived from North America, so the accuracy of the model is

307 higher in North Hemisphere, especially in Northern America.

### 308 **3.2 Validation with IGS tropospheric delay data**

309 IGS has provided final troposphere products with a temporal resolution of 5  
310 minutes since 1998. In 2010, some IGS sites have the severe problem of ZTD data  
311 missing. For a convinced validation, only the IGS sites with at least 120 days  
312 (approximately a third of the year) of tropospheric delays are selected. Consequently,  
313 Therethere are 362 IGS sites selected in 2010 to verify the accuracy of GZTD2 model,  
314 and the distribution of IGS sites is shown in Figure 5. The uncertainties of the ZTD  
315 products are very small (see Figure 5) with a mean value of 1.5 mm, indicating high  
316 quality of the ZTD products. Considering the ZTD products of IGS sites as true value,  
317 we tested and analyzed the ZTD estimates of GZTD2 model, GZTD model, EGNOS  
318 model and UNB series models. The Bias and RMS statistical results are shown in Table  
319 3.



320

321

**Figure 5.** Distribution of global IGS sites involved in validation

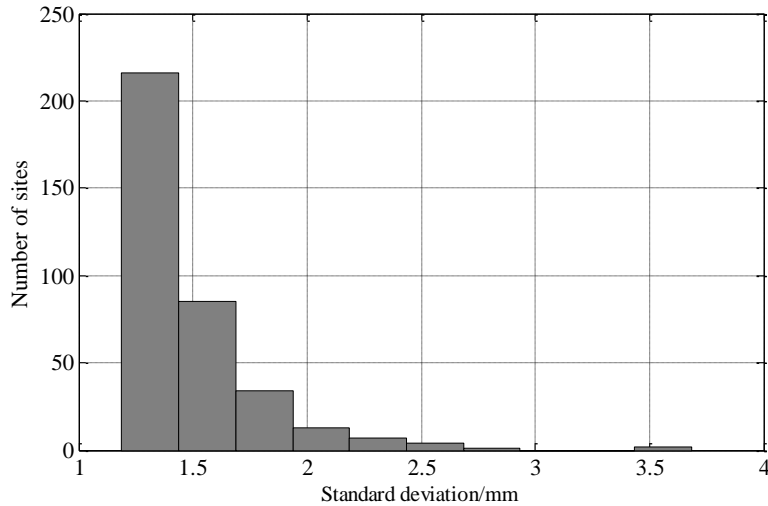
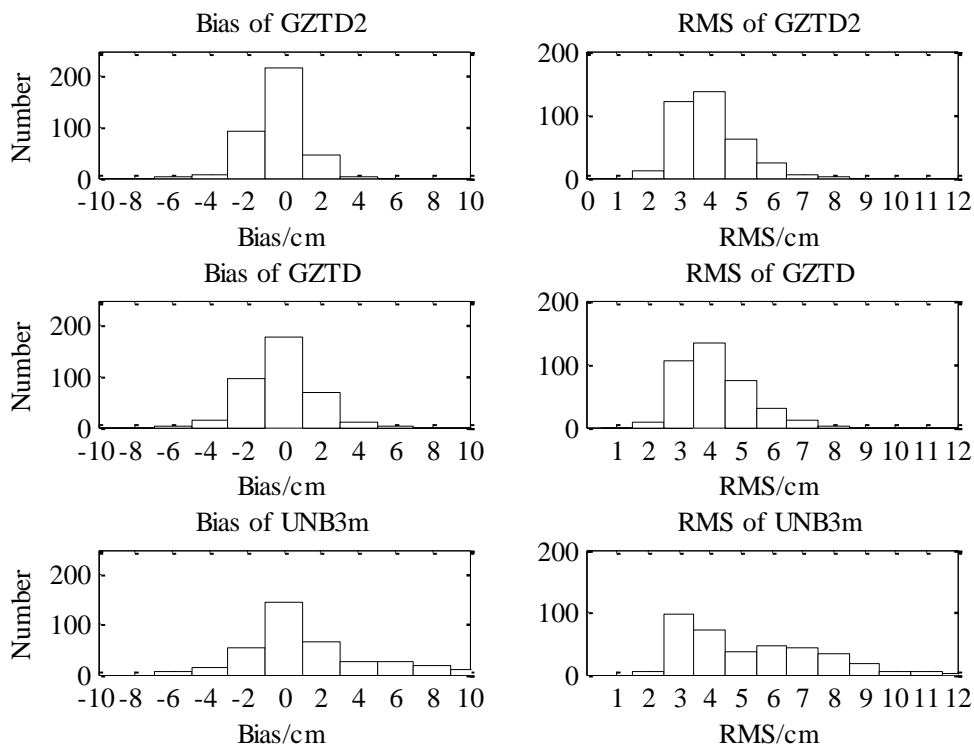


**Figure 6.** Histogram of uncertainty of ZTD at selected IGS sites

**Table 3.** Error of different considered models versus IGS data

	Bias (in cm)			RMS (in cm)		
	Mean	Min	Max	Mean	Min	Max
GZTD2	-0.3	-5.4	3.2	3.9	2.0	8.3
GZTD	-0.3	-6.0	5.1	4.2	2.1	8.5
UNB3m	1.2	-6.7	11.2	5.2	2.4	12.2
UNB3	2.6	-6.5	13.4	5.6	2.3	13.7
EGNOS	2.4	-6.6	15.3	5.7	2.4	12.3

325 As can be seen from Table 3, in terms of the results of accuracy and stability testing  
326 for all IGS sites throughout the year, GZTD2 model performs with the best average  
327 RMS, and then GZTD model follow~~ed~~<sup>ed</sup>. Global correction accuracy of the new model  
328 reaches centimeter level: Bias average value is -0.3 cm, average RMS is 3.9 cm.  
329 Compared with GZTD model, the range of Bias of GZTD2 model reduce by 2.4 cm  
330 and the maximum RMS of GZTD2 model decreases by 0.2 cm, indicating that the new  
331 model has a higher stability. Bias and RMS of EGNOS model are very close to those  
332 of UNB3 model and both are worse than UNB3m, which is similar to the results of Li  
333 et al. (2012). To display the correction effects of different models in a more intuitive  
334 way, we computed the distributions of Bias and RMS of all IGS stations. Figure 7 shows  
335 the histograms of Bias and RMS for the three models.



336

337

**Figure 7.** Histograms of Bias and RMS for three models

338

As can be seen from Figure 7, the Bias of GZTD2 model concentrates in range of  
 339 [-3cm 3cm], while the main distribution range of the Bias of GZTD model are 1cm  
 340 larger, and the Bias for UNB3m is distributed with the range more than 8 cm. It indicates  
 341 that GZTD2 model and GZTD model have small systematic deviations compared with  
 342 IGS data on a global scale, with the former performing better than the latter, but  
 343 problematic systematic deviations exist in the UNB3m model within some special areas.

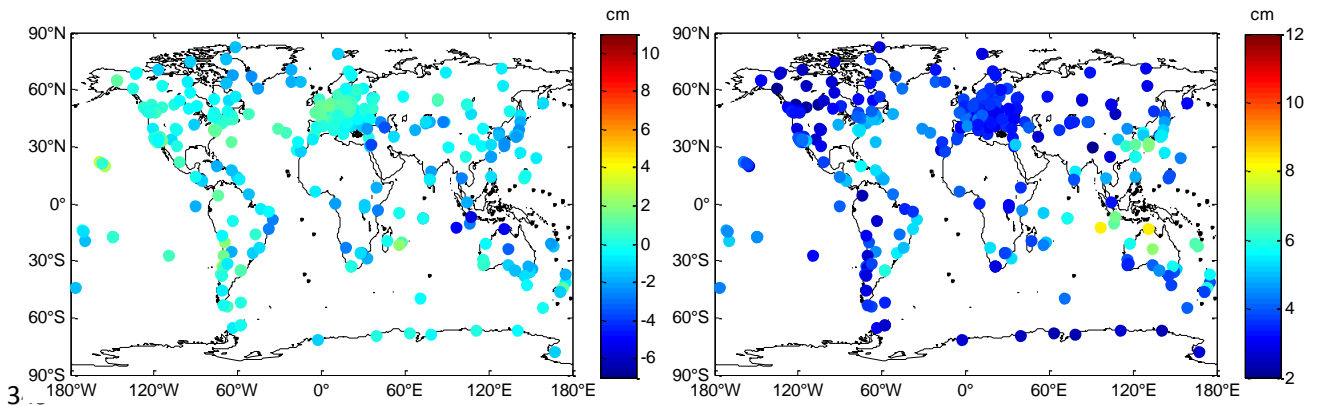
344

Figure 7 also shows that the RMS of GZTD2 model is mostly around 4 cm, whose  
 345 distribution is more concentrated compared to GZTD model, indicating GZTD2 model  
 346 has higher stability than GZTD. The RMS of UNB3m model are mainly around 5 cm

347

and exceed 9 cm at many sites, which further suggests the existence of systematic  
 348 deviations in certain areas in the UNB3m model.

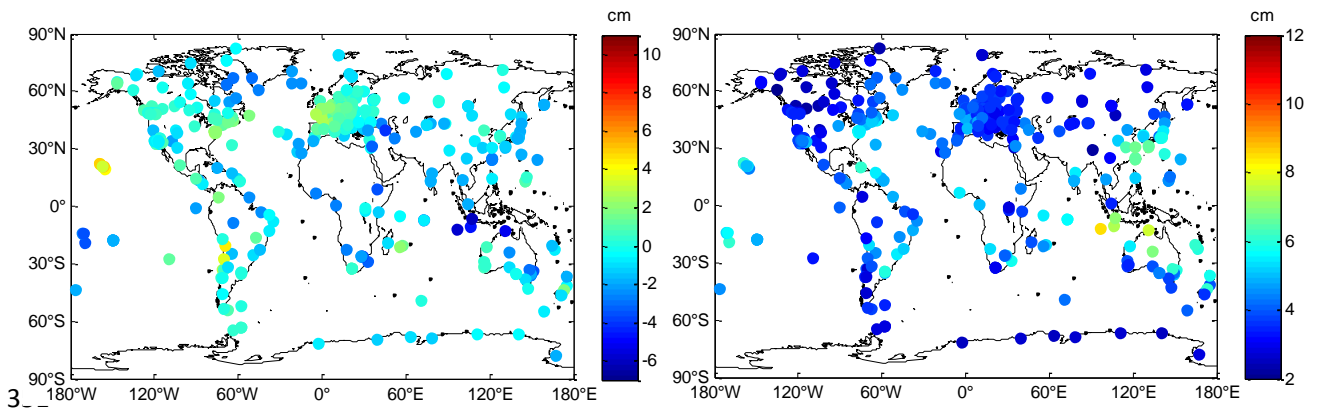
348



350

(a) GZTD2 Bias

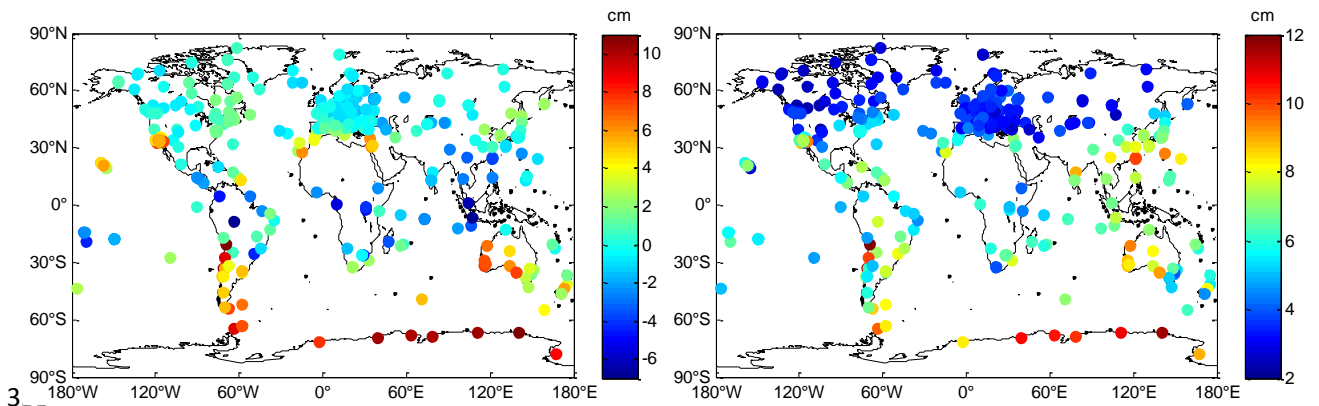
(b) GZTD2 RMS



352

(c) GZTD Bias

(d) GZTD RMS



354

(e) UNB3m Bias

(f) UNB3m RMS

355

**Figure 8.** Global distributions of Bias and RMS for different models

356

To further analyze the accuracy of the different models varying with location,

357

Figure 8 shows the global distributions of Bias and RMS calculated from different

358

models for IGS sites. As can be seen from Figure 8, GZTD2 and GZTD model largely

359

eliminate the effects caused by latitude and longitude variations, and the former is more

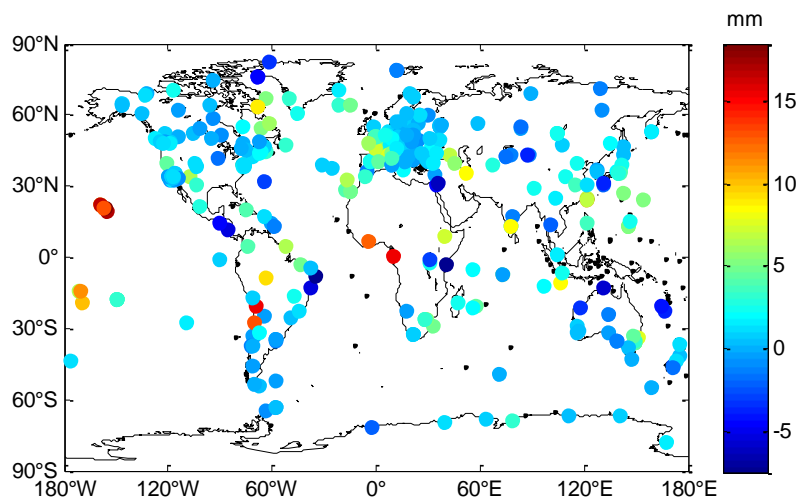
360

stable than the latter in terms of global distribution of Bias and RMS in spite of a few

361

sites with relative large error, of which most sites are located in the ocean and seacoast

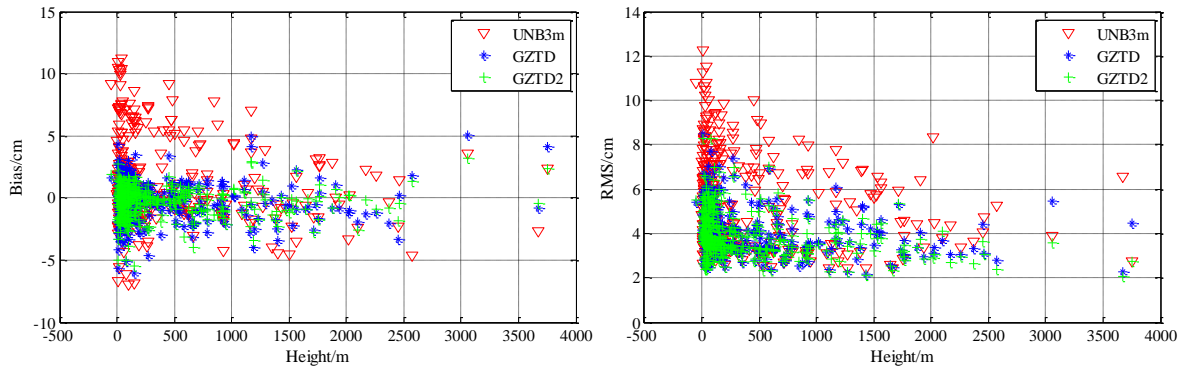
362 areas. A more clear comparison in terms of RMS between GZTD and GZTD2 is shown  
 363 in Figure 9. The ~~reduced~~ reduction for RMS can be found at most sites (the number is 273)  
 364 when moving from GZTD to GZTD2, which account for 75.4% of all sites. The  
 365 significant improvements of RMS are found at the sites in low-latitude areas such as  
 366 Pacific Ocean, South America coast and West Africa coast where the diurnal variations  
 367 are notable (see Figure 3d). This result proves the reasonability of adding diurnal  
 368 variations in GZTD2. For UNB3m model, as it is presented in Figure 8 Biases are  
 369 negative in most parts of the Northern Hemisphere and positive in most parts of the  
 370 Southern Hemisphere with significantly larger deviations, and RMS are smaller for  
 371 areas in the latitudes higher than 30 degrees, again suggesting that the correction effect  
 372 of UNB3m model is regional.



373  
 374 **Figure 9.** Global distribution of the difference between GZTD's RMS and GZTD2's RMS (GZTD's  
 375 RMS minus GZTD2's RMS)

376 Figure 10 shows the global distribution of Bias and RMS with respect to height  
 377 for GZTD2 model, GZTD model and UNB3m model. As can be seen, the Bias and  
 378 RMS are ~~larger~~ larger with height less than 500 m for all three models. Between 500m  
 379 and 2000m height, the Bias and RMS of GZTD model and GZTD2 model perform  
 380 better than that of UNB3m model, and the overall correction effects of the GZTD and  
 381 GZTD2 model are also better than the latter. Due to the same exponential function and  
 382 reducing constant for height, the distribution patterns of the Bias and RMS of GZTD  
 383 and GZTD2 model with respect to height are roughly similar, but the latter is obviously

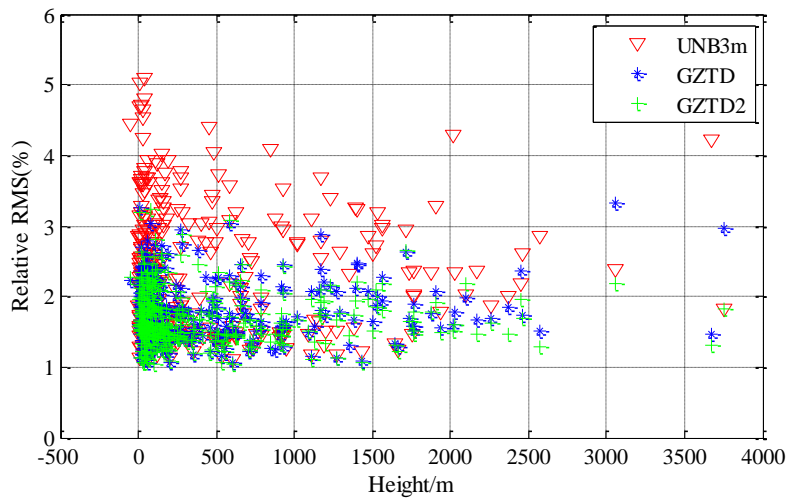
384 superior to the former.



385

386 **Figure 10.** Global distributions of Bias and RMS for different models with respect to height

387 For a more comprehensive analysis of the relationship between model stability and  
388 height, Figure 11 presents the global distribution of relative RMS for three models with  
389 respect to height. The relative RMS is the ratio of the RMS to the annual mean ZTD at  
390 the site. Basically, a relative accuracy between 1% and 2.5% can usually be stated for  
391 the majority of the sites from GZTD2 model, and the relative accuracy is less than 3%  
392 for GZTD model, showing that both perform better than UNB3m model.

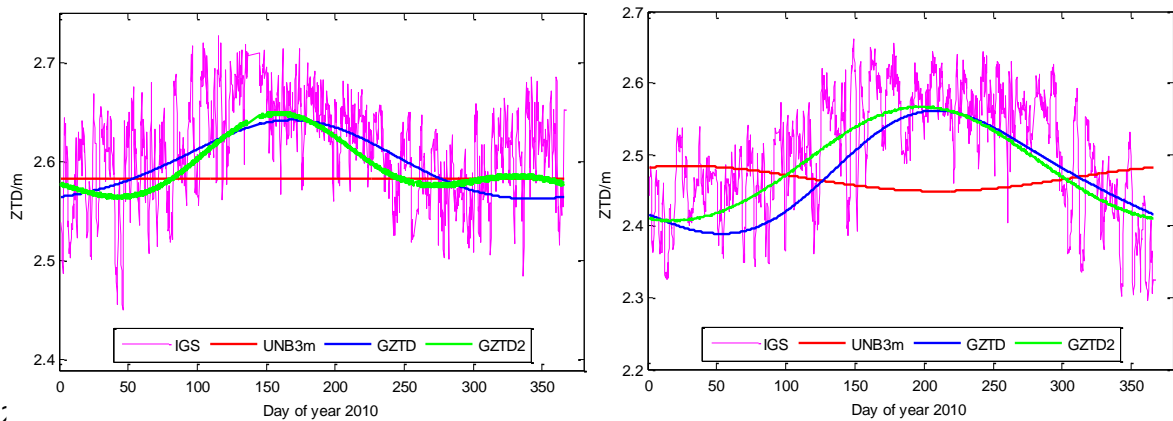


393

394 **Figure 11.** Relative RMS for different models with respect to height

395 Figure 12 illustrates the comparisons between IGS ZTD data and ZTDs  
396 determined by UNB3m, GZTD and GZTD2 models over the year 2010 at site KOUR  
397 and TWTF. During the whole year 2010, the ZTD values estimated by GZTD2 model  
398 show the best agreement with the IGS data, which are better than that of GZTD model  
399 without diurnal terms. The ZTDs determined by UNB3m model vary slightly  
400 throughout the year 2010, thus resulting in poor performance. The results in Figure 12

401 indicates that GZTD2 model has a temporal stability for correction accuracy.



402  
403 **Figure 12.** ZTDs at site KOUR (5.3°N, 52.8°W, 9.5m; left) and TWTF (24.9°N, 121.2°E, 189.9m;  
404 right) as provided by IGS and as estimated by different models over year 2010

405 From the above analysis, we can conclude that the overall accuracy of GZTD2  
406 model is up to centimeter level. GZTD2 model is ~~obviously~~substantially superior to  
407 other commonly used models in terms of Bias and RMS, and the accuracy  
408 ~~improve~~improves significantly compared with GZTD model, thus performing a higher  
409 reliability and stability.

410

## 411 **4. Conclusions**

412 ~~In this paper, we used time series data of global tropospheric zenith delays~~  
413 ~~provided by GGOS Atmosphere, and considered the diurnal variation in the ZTD based~~  
414 ~~on the GZTD model, and adopted a modified expansion function, and ultimately~~  
415 ~~developed an improved model named GZTD2. In this paper, using the time series data~~  
416 ~~of global tropospheric zenith delays provided by GGOS Atmosphere, we analyzed the~~  
417 ~~diurnal variation in the ZTD which is neglected in the previous GZTD model, then we~~  
418 ~~modified the model function to develop an improved model named GZTD2. We~~  
419 ~~conducted external validation testing with GGOS ZTD grid data which was not~~  
420 ~~involved in modeling, and IGS tropospheric product. The testing results of ZTD grid~~  
421 ~~data reflect the global precision and stability for GZTD2 model at four moments each~~  
422 ~~day, and the global average Bias and RMS for GZTD2 model are 0.2 cm and 3.8 cm~~

423 ~~respectively; the global average Bias is comparable to that of GZTD model, but the~~  
424 ~~global average RMS has been reduced by 3 mm; the Bias and RMS are far better than~~  
425 ~~EGNOS model and the UNB series models. The testing results of GGOS ZTD grid data~~  
426 ~~show that the global average Bias and RMS for GZTD2 model are 0.2 cm and 3.8 cm~~  
427 ~~respectively. The global average Bias is comparable to that of GZTD model, but the~~  
428 ~~global average RMS has been reduced by 0.3 cm. Both the Bias and RMS are far better~~  
429 ~~than EGNOS model and the UNB series models.~~ The testing results of global IGS  
430 tropospheric product show that the Bias and RMS for GZTD2 model are -0.3 cm and  
431 3.9 cm, superior to ~~that those~~ of GZTD (-0.3 cm and 4.2 cm), indicating higher accuracy  
432 and reliability compared to the EGNOS model and the UNB series models.

433 Overall, compared to GZTD model, GZTD2 model improves the temporal  
434 resolution and spatial resolution by considering diurnal periodic variations and  
435 modifying the expansion function, further completing and optimizing the theory of  
436 model establishment. The reliability and stability for GZTD2 model are much better  
437 than other commonly used models. However, like other empirical models such as  
438 UNB3m, GZTD2 model would be inaccurate in extreme weather events. Saastamoinen  
439 model is recommended if the real-time meteorological observations are available under  
440 extreme weather events. Moreover, GZTD2 model doesn't consider the semidiurnal  
441 variations due to the temporal resolution of GGOS data. In order to build a global  
442 tropospheric model with high accuracy, ZTD data with high quality and resolution are  
443 required, and the diurnal and semidiurnal variations as well as the subtle secular  
444 variation trend of ZTD need more detailed and further study.

445  
446 *Acknowledgements* The authors would like to express gratitude toward GGOS  
447 Atmosphere for providing related data. Great appreciation also goes to IGS for their  
448 data supporting of reference tropospheric product. This research was supported by the  
449 National Natural Science Foundation of China (41174012; 41274022) and The  
450 National High Technology Research and Development Program of China  
451 (2013AA122502) and the Fundamental Research Funds for the Central Universities  
452 (2014214020202) and the Surveying and Mapping Basic Research Program of

453 *National Administration of Surveying, Mapping and Geoinformation (13-02-09).*

454

## 455 **References**

456 Black H D (1978). An easily implemented algorithm for the tropospheric range correction. *Journal*  
457 *of Geophysical Research: Solid Earth (1978–2012)*, **83**(B4), 1825-1828.

458 B öhm, J., Heinkelmann, R., & Schuh, H. (2007). Short note: a global model of pressure and  
459 temperature for geodetic applications. *Journal of Geodesy*, **81**(10), 679-683.

460 B öhm, J., & Schuh, H. (eds.) (2013). *Atmospheric Effects in Space Geodesy*, Springer Verlag, ISBN  
461 978-3-642-36931-5.

462 B öhm, J., Möller, G., Schindelegger, M., Pain, G., & Weber, R. (2015). Development of an improved  
463 empirical model for slant delays in the troposphere (GPT2w). *GPS Solutions*, *19*(3), 433-441.

464 Byun, S. H., & Bar-Sever, Y. E. (2009). A new type of troposphere zenith path delay product of the  
465 international GNSS service. *Journal of Geodesy*, **83**(3-4), 1-7.

466 Collins J P, Langley R B(1997). *A tropospheric delay model for the user of the wide area*  
467 *augmentation system. Department of Geodesy and Geomatics Engineering*, University of New  
468 Brunswick.

469 Collins, J. P., & Langley, R. (1998, September). The residual tropospheric propagation delay: How  
470 bad can it get? In *PROCEEDINGS OF ION GPS* (Vol. 11, pp. 729-738). INSTITUTE OF  
471 NAVIGATION.

472 Dodson A H, Chen W, Baker H C, Penna N T, Roberts G W, Jeans R J, Westbrook J(1999).  
473 Assessment of EGNOS tropospheric correction model. In *Proceedings of the 12th International*  
474 *Technical Meeting of the Satellite Division of The Institute of Navigation (ION GPS 1999)* (pp.  
475 1401-1408).

476 Hopfield H S (1969). Two - quartic tropospheric refractivity profile for correcting satellite data.  
477 *Journal of Geophysical research*, **74**(18), 4487-4499.

478 Jin, S., Park, J. U., Cho, J. H., & Park, P. H. (2007). Seasonal variability of GPS - derived zenith  
479 tropospheric delay (1994 - 2006) and climate implications. *Journal of Geophysical Research:*  
480 *Atmospheres (1984 - 2012)*, 112(D9).

481 Jin, S., Luo, O. F., & Gleason, S. (2009). Characterization of diurnal cycles in ZTD from a decade  
482 of global GPS observations. *Journal of Geodesy*, **83**(6), 537-545.

483 Krueger E, Schueler T, Hein G W, Martellucci A, Blarzino G(2004, May). Galileo tropospheric  
484 correction approaches developed within GSTB-V1. In *Proc. ENC-GNSS*.

485 Krueger E, Schueler T, Arbesser-Rastburg B(2005). The standard tropospheric correction model for  
486 the European satellite navigation system Galileo. *Proc. General Assembly URSI*.

487 Lagler, K., Schindelegger, M., Böhm, J., Krásná H., & Nilsson, T. (2013). GPT2: Empirical slant  
488 delay model for radio space geodetic techniques. *Geophysical research letters*, **40**(6), 1069-1073.

489 Leandro R, Santos M C, Langley R B(2006, January). UNB neutral atmosphere models:  
490 development and performance. In *ION NTM* (pp. 18-20).

491 Leandro R F, Langley R B, Santos M C(2008). UNB3m\_pack: a neutral atmosphere delay package  
492 for radiometric space techniques. *GPS Solutions*, **12**(1), 65-70.

493 Li Wei, Yuan Y B, Ou J K, Li H, Li Z S(2012). A new global zenith tropospheric delay model  
494 IGGtrop for GNSS applications. *Chinese Science Bulletin*, **57**(17), 2132-2139.

495 Li, Wei, Yuan, Y., Ou, J., Chai, Y., Li, Z., Liou, Y. A., & Wang, N. (2015). New versions of the  
496 BDS/GNSS zenith tropospheric delay model IGGtrop. *Journal of Geodesy*, **89**(1), 73-80.

497 Möller, G., Weber, R., & Böhm, J. (2014). Improved troposphere blind models based on numerical  
498 weather data. *Navigation*, **61**(3), 203-211.

499 Penna N, Dodson A, Chen W(2001). Assessment of EGNOS tropospheric correction model. *The*  
500 *Journal of Navigation*, **54**(01), 37-55.

501 Pramualsardikul, S., Haas, R., Elgered, G., & Scherneck, H. G. (2007). Sensing of diurnal and  
502 semi - diurnal variability in the water vapour content in the tropics using GPS measurements.  
503 *Meteorological Applications*, **14**(4), 403-412.

504 Saastamoinen J (1973). Contributions to the theory of atmospheric refraction. *Bulletin Géodésique*  
505 *(1946-1975)*, **107**(1), 13-34.

506 Schüler T (2014). The TropGrid2 standard tropospheric correction model. *GPS solutions*, **18**(1),  
507 123-131.

508 Spilker, J. J. (1980). GPS signal structure and performance characteristics. *Global positioning*  
509 *system*, **1**, 29-54.

510 Trenberth, K. E., Fasullo, J., & Smith, L. (2005). Trends and variability in column-integrated

511 [atmospheric water vapor. \*Climate Dynamics\*, 24\(7-8\), 741-758.](#)

512 Ueno M, Hoshino K, Matsunaga K, Kawai M, Nakao H, Langley R B, Bisnath S B (2001, January).

513 Assessment of atmospheric delay correction models for the Japanese MSAS. In *Proceedings of*

514 *the 14th International Technical Meeting of the Satellite Division of The Institute of Navigation*

515 *(ION GPS 2001)* (pp. 2341-2350).

516 Uppala S M, Källberg P W, Simmons A J, Andrae U, Bechtold V, Fiorino M, ... , Woollen J (2005).

517 The ERA - 40 re - analysis. *Quarterly Journal of the Royal Meteorological Society*, **131**(612),

518 2961-3012.

519 Yao Y B, He C Y, Zhang B, Xu C Q(2013). A new global zenith tropospheric delay model GZTD.

520 *Chinese Journal of Geophysics-Chinese Edition*, **56**(7), 2218-2227,doi:10.6038/cjg20130709